

Fig. 3

for planar theory. If the initial tumbling rate is very high, the satellite will indeed tumble after rod extension. For lower initial tumbling rates, the satellite may capture for a while, then tumble, capture again, etc. It is best to examine capture in the light of the initial tumbling that the satellite may be expected to have.

The satellite will be injected into orbit either from a spin-stabilized final propulsion stage or from one having its own attitude stabilization. If the final propulsion stage is spin-stabilized, the satellite is despun by discharging gas or releasing yo-yo weights before extending the tubes. Before extending the tubes, such a satellite will be tumbling about any axis with a rate of 1 rpm typically. Most of this tumbling rate originally came from misalignment of the thrust vector during spin-up, with the rest coming from the separation mechanism.

If the final propulsion stage has its own attitude stabilization, the satellite before extending its tubes will be tumbling about any axis with a rate of 0.1 rpm typically.

The satellite's motions for an initial rate of 1 rpm are shown in Fig. 3 (middle). At time 0 the tubes are released. At time $\frac{1}{2}$ hr, the tubes are fully extended 150 ft, measured outward from the central payload. The motion is shown by giving the earth pointing error, the angle between the satellite's yaw axis and the local vertical. The initial rate is referenced to inertial space. For Fig. 3 (middle) the initial rate is evenly divided among pitch, roll, and yaw, and the pitch rate is "positive." A positive pitch rate as seen from inertial space is in the same direction as that of the satellite orbiting the earth. The direction of the pitch rate is important for determining whether the satellite captures without damping. It is also important for determining whether it captures with damping, for certain types of damping.

For Fig. 3 (middle) the satellite is captured, since the angle the yaw axis makes with local vertical remains less than 90° . If the 1-rpm initial rate has a negative rather than positive pitch component, it also is captured.

By raising the total rate to 4 rpm with equal components in pitch, roll, and yaw, and a negative pitch rate, the satellite is no longer captured, as seen in Fig. 3 (top). Thus, for initial tumbling rates to be anticipated (up to 1 rpm), the satellite has a good chance of capture at an orbital altitude of 5000 naut miles.

It is sufficient to use the phrase "good chance" of capture. There is no justification for precisely defining the bounds of

the capture map until damping is accounted for. All passively stabilized satellites must have some form of damping. Damping will superimpose on the basic capture phenomenon discussed, an added effect converting the initial tumbling to some other motion. The effect depends on the particular damping technique employed, and it is only when the technique has been specified that a precise capture map has mission significance.

Effect of Nose Bluntness on the Flow around a Typical Ballistic Shape

DONALD W. EASTMAN* AND LEONARD P. RADTKE†
The Boeing Company, Seattle, Wash.

THE purpose of this note is to show the effects of nose bluntness on the flow around a typical ballistic shape. Theoretical and experimental results are presented.

Four blunt cone-cylinder-flare combinations tested at $M = 6.10^4$ are shown in Figs. 1-4. The bodies are identical except for the amount of hemispherical nose bluntness. The pressure coefficients measured along the surface of the bodies and the shock shapes obtained from schlieren photographs also are shown. The total temperature and pressure during the test were 550°F and 900 psia, respectively.

A method of characteristics program² was used to calculate the flow fields around these bodies. This program has the capability to calculate and cross shock waves caused by flares or flow recompression. Without the capability to calculate recompression shocks, the program would "blow up" at the start of the shock. This type of calculation is probably the most difficult of any connected with the calculation of flow around axisymmetric bodies. Because of the low total temperature of the experiments, an ideal gas with $\gamma = 1.4$ was used for all calculations. The subsonic nose region was calculated using an inverse method program.

Figures 1-4 show a comparison of experimental and theoretical results. Except for the flare region there is an excellent comparison between the two.

Figure 2 illustrates an interesting phenomenon associated with flow around blunt cones. That is, the shock wave caused by the recompression of the flow along the nose cone. If the cone were very long, the pressure eventually would reach the sharp cone value. Since this value is higher than the pressure aft of the blunt nose, the flow must recompress. Thus, the recompression shock is formed. This shock could not be seen in the schlieren photographs. Its effect on the bow shock can be seen, however, by examining Fig. 2 carefully. When the recompression shock intersects the bow shock, the bow shock wave angle increases approximately 1.5° .

Referring to Figs. 1-4, it can be seen that the pressure distribution along the flare definitely is influenced by the amount of nose bluntness. In fact the flare pressures for the sharp body are about twice the values of the completely blunt body. Figures 2-4 show how the high entropy layer from the blunt nose reduces the pressure near the flare juncture. For the slightly blunted body (Fig. 2) the layer is thin, and the pressure distribution aft of the juncture starts to increase to the sharp nose value of Fig. 1. Bluntness effects dominate the flow over the flare in Figs. 3 and 4. However, the

Received June 24, 1963.

* Research Engineer, Aero-Space Division, Flight Technology Department. Member AIAA.

† Research Engineer, Aero-Space Division, Applied Mathematics Organization. Member AIAA.

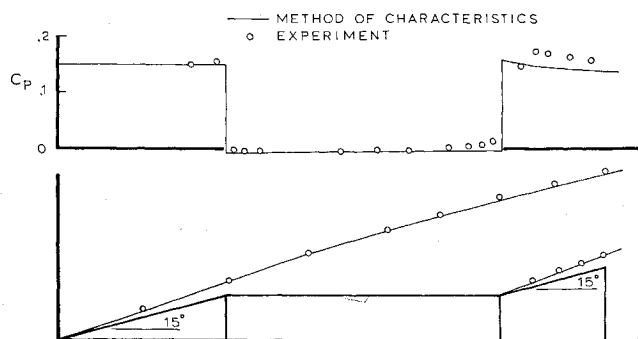


Fig. 1 Pressure distribution and shock shapes on the sharp nosed body, $r_n/r_b = 0$.

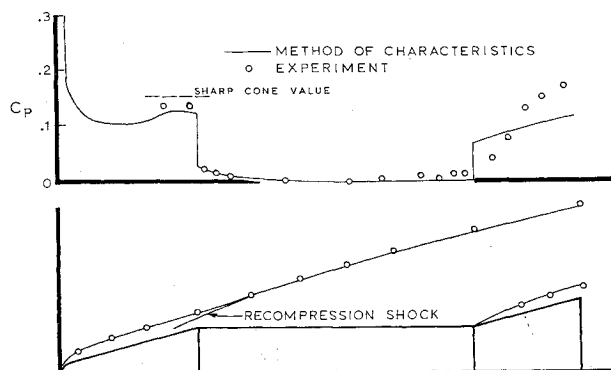


Fig. 2 Pressure distribution and shock shapes on the slightly blunted body, $r_n/r_b = 0.2273$.

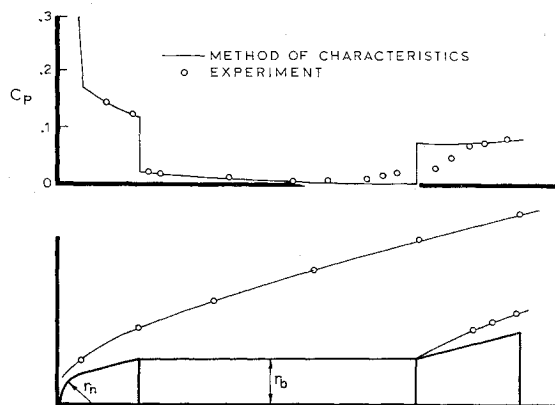


Fig. 3 Pressure distribution and shock shapes on the moderately blunted body, $r_n/r_b = 0.6825$.

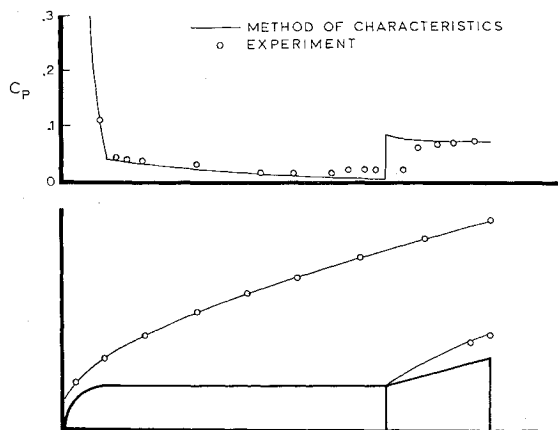


Fig. 4 Pressure distribution and shock shapes on the completely blunted body, $r_n/r_b = 1.0$.

pressure at the rear of the flare in Fig. 3 has started to increase to the sharp nose value.

The figures presented also illustrate the effect of separation on the pressure near the flare juncture. Figure 2 shows that separation can cause pressures on the flare to be considerably higher than the theoretical values. Separation was indicated clearly in the schlieren photographs, and also the flare shock waves were not attached to the body. A thorough study of separation is currently being conducted and, therefore, is not treated here.

References

- 1 Tauber, M. E., "Pressure distributions on a series of blunted cone-cylinder-flare configurations," Boeing Co. Document D2-10596 (1962).
- 2 Eastman, D. W., "Two dimensional or axially symmetric real gas flows by the method of characteristics, Part II: Flow fields around bodies," Boeing Co. Document D2-10598 (1963).

Penetration of Spacecraft by Lunar Secondary Meteoroids

WILLARD S. BOYLE* AND G. TIMOTHY ORROK†
Bellcomm Inc., Washington, D. C.

IT is recognized that the flux of meteoroids in cislunar space is sufficiently large that it must be taken into account in designing the protective skin of a spacecraft.¹ Recent studies at the Ames Laboratory reported by Gault, Shoemaker, and Moore² on hypervelocity impact processes have shown that the total mass ejected by a hypervelocity particle may exceed the mass of the incident particle by several orders of magnitude. This has raised the question as to whether the secondary meteoroids generated at the lunar surface might not appreciably increase the probability of puncture of a spacecraft when it is exposed to this secondary flux. It should be noted that 1) in traversing the ejecta cloud, the spacecraft itself may determine the mean impact velocity, and 2) the question of a "captured flux," or meteoroid concentration near the moon, is not settled. The purpose of this note is to examine, on rather general grounds, the problem of the spacecraft at rest on the lunar surface and to set limits on the enhanced probability of puncture.

The basic argument is that the total kinetic energy available to be distributed to the secondary particles is bounded by the kinetic energy of the primary particle. This allows us to write down rather powerful restrictions on the integrated energy spectrum of the secondary particles and, in particular, to derive the increase in the flux of particles exceeding a given energy. The assumption is made that the thickness of protective skin penetrated by a particle depends only on the kinetic energy,¹⁻³ and hence it is shown that the probability of puncture is, at most, increased by a small factor. We now proceed with the argument.

Kinetic energy is, at most, conserved in a primary impact. The secondary particles, whatever their combined mass, share the incident energy. This process could double the energy flux incident on the moon. The arguments in this paper require that there be few tertiary particles capable of puncturing a spacecraft, i.e., that the energy flux cannot be more than doubled. The velocities of the secondaries must be quite small. First, the mass-multiplication in the impact is very large; to balance this, the mean velocities must be

Received July 18, 1963.

* Director, Space Science and Exploratory Studies Division.

† Member of Technical Staff, Space Science and Exploratory Studies Division.